Infrared Absorption Studies of *n*-Heptane under High Pressure

Masashi Yamaguchi, Scott V. Serafin, Thomas Hellman Morton, and Eric L. Chronister*

Department of Chemistry, University of California, Riverside, California 92521-0408

Received: September 25, 2002; In Final Form: December 9, 2002

Mid-infrared spectra of neat *n*-heptane at room temperature are presented over a pressure range from ambient to 70 kbar. The application of hydrostatic pressure induces frequency shifts, band splittings, and significant changes in the line shapes of internal vibrational modes both in liquid and in solid phases. The results are discussed in terms of the liquid−solid phase transition and changes of the population of molecular conformers. Evidence for a solid−solid phase transition near 30 kbar is also presented.

Introduction

The phase behavior and the conformational equilibria of simple saturated hydrocarbons have attracted considerable attention for many years and have been investigated extensively.[1−6] Standard textbooks point out the effects of molecular symmetry, whereby the melting points of *n*-alkanes with even and odd numbers of carbons trace out two distinct curves. The odd homologues melt at lower temperatures than would be predicted by interpolating between even homologues, a result attributed to the fact that, when fully extended, chains with an even number of carbons possess inversion symmetry, while chains with an odd number of carbons do not.[7] As a consequence, the former pack better in a crystal than do the latter. By contrast, no such differences between even and odd *n*-alkanes are apparent in the liquid phase, because the boiling points increase in a smooth progression with increasing molecular weight.

The properties of alkyl chains are fundamentally important for understanding a variety of phenomena in biology and polymer science, such as the phase behavior of highly ordered lipid−hydrocarbon chain assemblies[8,9] and the morphology and crystal growth of polymers.[10,11] Vibrational spectroscopy is a powerful tool for investigating conformation and dynamics of molecules in condensed phases and has been used extensively.[12−14] Application of hydrostatic pressure to molecular systems that are held together by van der Waals interactions modifies the balance of the intra- and intermolecular forces as a result of changes in the distances between molecules. For linear alkanes, which have many intramolecular degrees of freedom, the application of pressure perturbs the distribution of molecular conformations in the liquid phase.[3,12,15,16] It has been proposed that the application of pressure increases the population of globular conformers with gauche bonds. Schoen et al.[15] reported high-pressure Raman experiments on liquid *n*-hexane, *n*-heptane, and *n*-octane, all of which exhibited a pressure dependence of the Raman intensity of longitudinal acoustic modes. From their data, they deduced the pressure dependence of the molecular conformational populations. Kato et al.[12] reported the pressure dependence of infrared spectra of *n*-pentane and discussed its conformational equilibrium in terms of the spectroscopic line shape changes for the methyl rocking mode in the liquid phase. In addition, the pressure dependence of the low-temperature dynamics of dye-doped solid *n*-alkane crystals has been studied by hole burning experiments, and it has been reported that they have unusually large pressure-induced broadening.[17] Investigation under high pressure is desirable to further understand the phase behavior as well as the dynamics of these molecular systems.

CHART 1. Orientations about a Single Bond

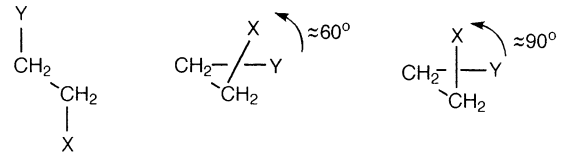

antiperiplanar or *trans* (**A**) *synclinal* or *gauche* (**G**) *ortho* (**O**)

In this article, we present the results of an infrared study of *n*-heptane under high pressure. The *n*-heptane molecule has a sufficiently long chain to take on a variety of conformations, some of which are spectroscopically distinguishable. We have investigated the effect of pressure on the infrared spectrum of *n*-heptane in the liquid and solid phase up to 70 kbar by using a diamond anvil cell, and we interpret the results with the help of a density functional theory (DFT) survey of low-lying molecular conformations. The pressure-induced frequency shifts, band splittings, and changes in line shape are discussed in terms of the liquid−solid phase transition and the population of conformational isomers.

Various nomenclature systems have been used to describe chain conformations. The two most commonly seen orientations are represented at the center and left in Chart 1, and three different designations for each are summarized. When the substituents X and Y are CH_2 or CH_3 groups, the nonbonded interactions between their hydrogens are repulsive, and the synclinal orientation is said to be gauche. This paper will follow a recently proposed recommendation that the ≈180° orientation be abbreviated as **A** and the ≈60° orientation be abbreviated as **G**. In some cases, the dihedral angle is closer to 90°. The proposed nomenclature for such an orientation is ortho (abbrviated as **O**).[18]

Note that the gauche and ortho geometries cannot be superimposed on their mirror images. Hence, the helical sense

* Author to whom correspondence should be addressed. E-mail: eric.chronister@ucr.edu. Phone: 909-787-3288. Fax: 909-787-3420.

10.1021/jp0221439 CCC: $25.00
Published on Web 03/06/2003

of a specific case should be indicated: $\mathbf{G}_-$ versus $\mathbf{G}_+$ (or $\mathbf{O}_-$ versus $\mathbf{O}_+$).[18]

In saturated hydrocarbons, an isolated **G** is less stable than an **A** by approximately $\Delta H \approx 3.5$ kJ mol^{-1}. Nevertheless, gauche bonds are quite abundant, largely for statistical and entropic reasons. A fully extended *n*-alkane (all **A** or all trans) has both a C_2 axis and a plane of symmetry. When the chain has more than four carbons, introducing one **G** removes both symmetry elements, increasing the entropy by $2R$ ln 2 (R ln 2 from entropy of mixing $\mathbf{G}_-$ and $\mathbf{G}_+$ and R ln 2 from third law entropy). Thus, at room temperature in the gas phase, the free energy change is small, $\Delta G \approx 0$, for interconverting a mixture of $\mathbf{G}_-$ and $\mathbf{G}_+$, with the fully extended conformation. Taking chains with more than one **G** into account, it has been estimated that the net number of single bonds in the vapor with **A** orientation in *n*-heptane vapor is about 2.25 times as great as the net number with **G** orientation.[19] However, the liquid contains a higher proportion of gauche bonds. X-ray diffraction of liquid *n*-heptane at 294 K and 1 atm pressure suggests that **A** and **G** bonds exist in a 55:45% (±8%) equilibrium.[20] In other words, nearly half of the CH_2-CH_2 bonds in liquid *n*-heptane are gauche, and this fraction increases with pressure[14] until the onset of solidification, at which time all the bonds become antiperiplanar (i.e., trans). This paper explores a comparatively simple model to account quantitatively for conformer distributions in the liquid.

Hydrocarbon chains with more than one **G** often exhibit intramolecular interactions, which imply that the energetic and entropic effects need not be strictly additive. For example, chains containing $\mathbf{G}_+$ and $\mathbf{G}_-$ adjacent to one another are not stable and revert to a high energy $\mathbf{G}_+\mathbf{O}_-$ or an $\mathbf{O}_+\mathbf{G}_-$ motif.[21] In the case of hexane, the proportions of **G** and **A** bonds (30:70%) predicted by ab initio computations agree with vapor phase predictions based on an empirically derived force field. We inquire as to whether the relatively large fraction of gauche bonds in liquid *n*-heptane can be accounted for in terms of conformational equilibria calculated using DFT.

Experimental Section

n-Heptane (Mallinckrodt) was used without further purification. A Merrill−Basset[22] type diamond anvil cell with a diamond culet size of 1 mm was used to generate high pressure up to 70 kbar. *n*-Heptane was placed between the diamond anvils (type IIa) together with a stainless steel gasket. The thickness of the gasket was 25 μm with a sample diameter of 500 μm. The pressure was determined by the ruby R_1-line fluorescence method with accuracy of about ±0.5 kbar. Infrared radiation was focused onto the sample with a gold-coated reflective objective. All infrared absorption spectra were measured on a Bruker HR-120 Fourier transform IR spectrometer at room temperature with a mid-IR light source (Globar) and a liquid nitrogen cooled mercury−cadmium−telluride detector. Each spectrum was accumulated for 1000 scans and averaged with resolution of 0.5 cm^{-1}.

DFT calculations were performed on all the heptane conformers having two or more antiperiplanar (trans) bonds, as well as for the two conformers having three gauche bonds of the same helicity, using GAUSSIAN98 at the B3LYP/6-31G* level. Normal modes, zero point energy differences, and ΔS_{vib} values are based on unscaled vibrational frequencies. The small differences in heat capacities of different conformers were neglected in calculating the free energy differences between them. Normal modes were animated using GaussView. DFT-calculated IR absorption intensities were used without scaling.

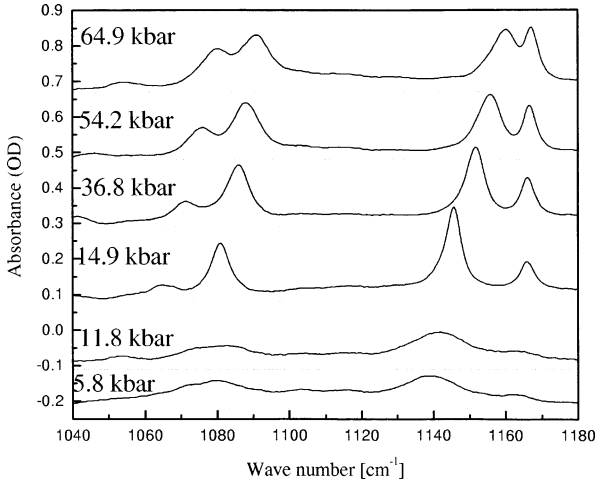

Figure 1. Infrared spectra of *n*-heptane in C−C stretching region at various pressures.

Results

C−C Skeleton Stretch Region. The infrared spectra of neat *n*-heptane were measured as a function of pressure up to 70 kbar. Representative spectra in the 1040−1180 cm^{-1} region are shown in Figure 1. The changes in the general character of the spectra between 11.8 and 14.9 kbar are due to the pressure-induced liquid−solid phase transition. The broad and weak absorption bands in the spectra at pressures >11.8 kbar become sharper, and significant frequency shifts are clearly observed between 11.8 and 14.9 kbar. In the solid phase, the fully extended (**AAAA**) conformation is considered dominant. The assignments of the bands corresponding to the **AAAA** conformation are shown in Table 1. The three intense peaks in Figure 1 that blue shift with pressure (i.e., 1065, 1080, and 1145 cm^{-1} at 14.9 kbar) have been mainly assigned to C−C skeleton stretching motions[23,24] in the solid phase. The frequency for the peak near 1165 cm^{-1} is attributed to a combination of CH_2 and CH_3 rocking and torsional motion[23,24] in the solid and shows little shift with pressure. The pressure dependence of the vibrational frequencies of the four bands in Figure 1 is plotted as a function of pressure in Figure 2. The clear discontinuity in the pressure shift of the absorption bands between 11.8 and 14.9 kbar is attributed to the liquid−solid phase transition. Liquid *n*-heptane contains a mixture of several different conformers. The frequencies in the solid do not necessarily correlate with the closest vibrational band in the liquid, because the pressure-dependent shifts in the liquid can come from changes in the populations of different conformers. Figure 3 shows representative spectra in the liquid phase for the C−C skeleton stretching region. The asymmetric line shape and increased shoulder bands observed for the high-pressure liquid are attributed to the existence of multiple conformational isomers (Figure 3), in contrast to the relatively sharp and symmetric features of the peaks in the solid state (Figure 1). The frequency change with pressure in the liquid is relatively small compared to the solid state. The most prominent pressure change in the liquid is the increase in band intensity near 1055 cm^{-1}, as indicated by an arrow in Figure 3. The multicomponent broad peak around 1080 cm^{-1} also changes its line shape with pressure due to changes in the relative intensities of its components.

CH_2 and CH_3 Twisting−Bending Region. Figures 4 and 5 show the CH_2 and asymmetric CH_3 bending−twisting region (1400−1550 cm^{-1}) in the IR spectra of *n*-heptane. The spectroscopic changes seen between 11.8 and 14.9 kbar (as in

TABLE 1: Vibrational Frequencies of *n*-Heptane in the Solid Phase in the 700−1500 cm^{-1} Domain for the AAAA Conformation[a]

obs freq (cm^{-1})[b]	DFT (cm^{-1})	obs freq (cm^{-1})[c]	VFF (cm^{-1})[d]	assignment
737.8	740	720 (s)	722	CH_2 rocking−(twisting)
769.8	783	766 (m)	766	CH_2 rocking−(twisting)
886.1	888	877 (m)	874	CH_3 rocking
912.0	925	911 (m)	911	CH_3 rocking
924.9	951	925 (m)	924	CH_2 rocking
1064.7	107,1073	1058 (m)	1057	C−C stretching
1081.1	1099	1075 (m)	1074	C−C stretching
1145.7	1166	1142 (m)	1144	C−C stretching
1165.9	1222	1177 (w)	1177	CH_2 twisting−(rocking)
1375.5	1356		1370	CH_2 rocking
1379.3	1389		1374	CH_2 wagging
1450.2	1441, 1442	1448 (m)	1446	asymm - CH_3 bending & CH_2 bending
1463.2	1515, 1525	1458 (m)	1461	asymm - CH_3 bending & CH_2 bending
1479.6	1529	1475 (s)	1472	symm - out-of-plane CH_3 bending

[a] Assignments are based on animation of DFT normal modes (VFF: Valence force field calculation (ref 24)). [b] This work (300 K and 14.9 kbar). [c] Reference 18 (77 K and 0 kbar). [d] Reference 24.

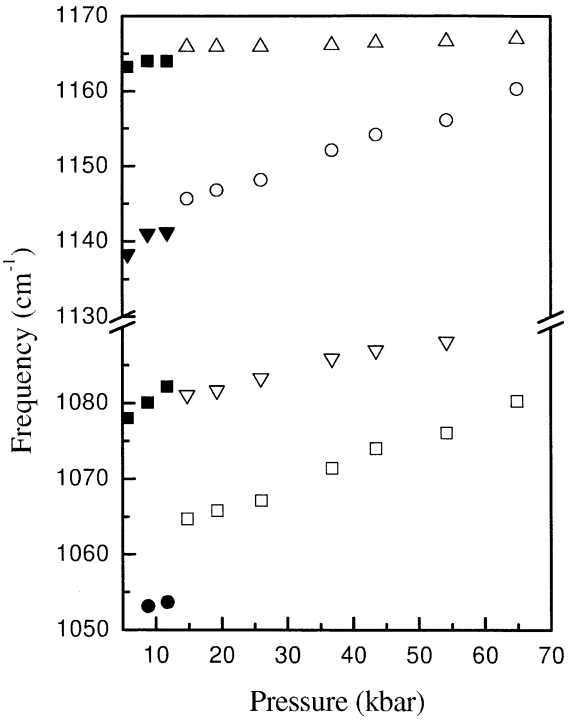

Figure 2. 2. Pressure dependence of the infrared peak frequency in C−C stretching region.

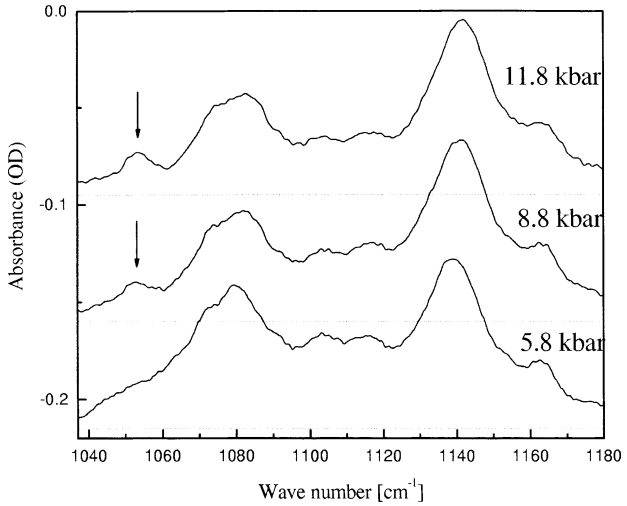

Figure 3. Expansion of infrared spectra of *n*-heptane in C−C stretching region at various pressure (liquid state).

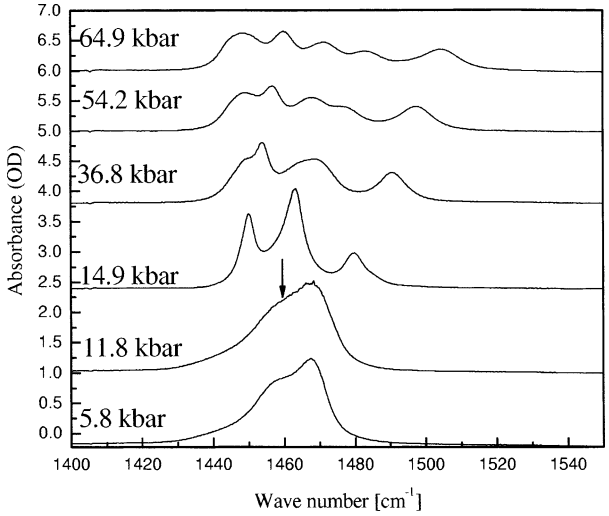

Figure 4. Infrared spectra of *n*-heptane in CH_2 and CH_3 twisting−bending at various pressure.

the C−C skeleton region described above) are due to the liquid−solid phase transition. The broad band consists of a multicomponent absorption observed for the liquid in Figure 4, which splits into three relatively sharp peaks above 14.9 kbar. The assignments of these peaks are given in Table 1, together with the results of a valence force field calculation for the fully extended (**AAAA**) conformation in the crystal by Snyder et al.[23] On one hand, increased pressure in the solid phase splits the peaks located near 1450 and 1460 cm^{-1} (at 14.9 kbar), as seen in Figure 4. On the other hand, the peak near 1480 cm^{-1} (at 14.9 kbar) does not show noticeable splitting as pressure increases. In the liquid, pressure-induced changes in the shape of the broad band are characterized by increased relative intensity near 1460 cm^{-1}, as indicated by an arrow in Figure 4. The peak position and the line width do not show significant changes with pressure in the liquid phase. The pressure effects on the bending region of the spectra in the liquid are due to relative changes in the conformational isomers rather than anharmonic effects, similar to the analysis of the C−C stretching region. The effects of pressure on the vibrational bands in this region are plotted in Figure 5.

CH_2 CH_3 Rock and Torsion Region. Figure 6 shows the pressure dependence of spectrum in the CH_2 and CH_3 rocking

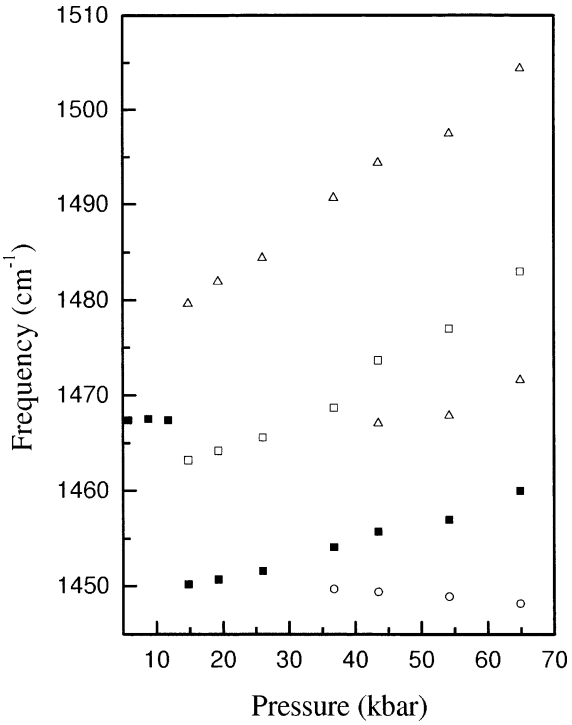

Figure 5. Pressure dependence of the infrared peak frequency in CH_2 and CH_3 twisting−bending region.

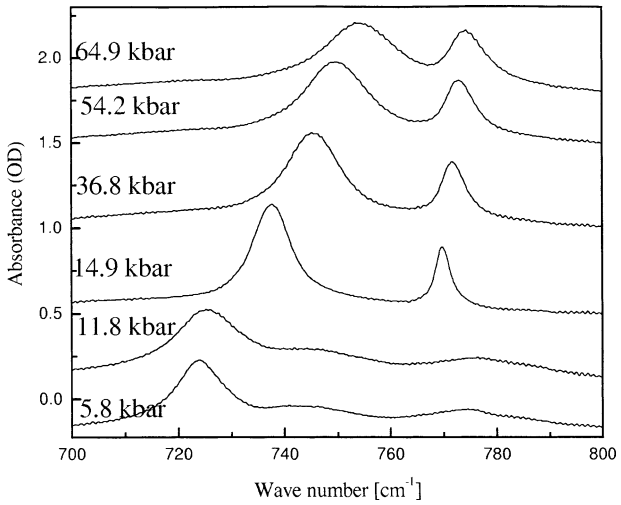

Figure 6. Infrared spectra of *n*-heptane in CH_2 rock and twist region at various pressure.

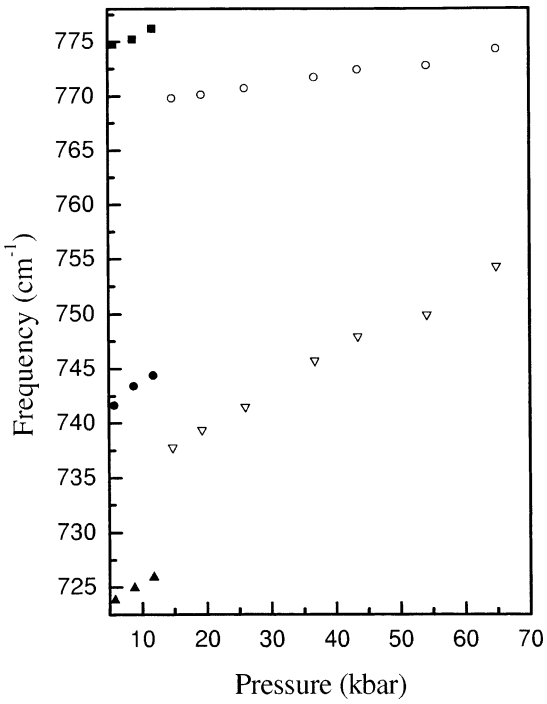

Figure 7. Pressure dependence of the infrared peak frequency in CH_2 rock and twist region.

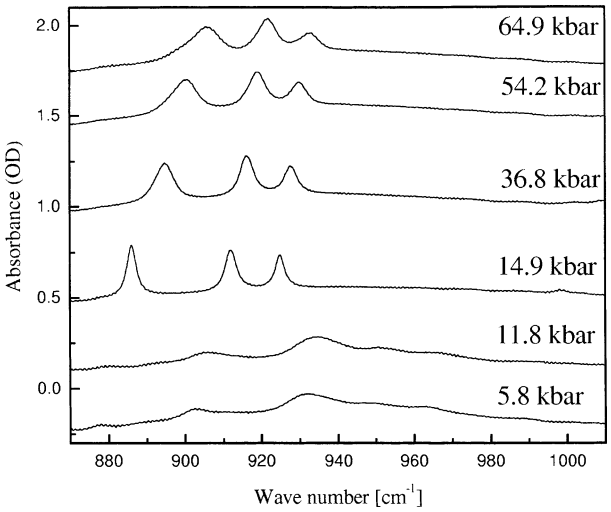

Figure 8. Infrared spectra of *n*-heptane in CH_3 rock region at various pressures.

mode region. Three broad peaks in the liquid phase become two relatively sharp peaks in the solid. The pressure dependence of the lower frequency peak has a much larger pressure dependence, as shown in Figure 7. Figures 8 and 9 show the pressure dependence of the IR spectrum in the 870−1100 cm^{-1} domain. The band near 880 cm^{-1} (at 14.9 kbar) shows a relatively large pressure dependence of its frequency compared to other bands in the solid-state spectrum in this region. The line widths of three distinct peaks in the solid (at 14.9 kbar) broaden as pressure increases.

Discussion

The pressure effects in the liquid phase are attributed to redistribution of conformational isomers rather than anharmonic pressure shifts of individual vibrational modes. Vibrational frequencies shift abruptly when the liquid solidifies. The pressure sensitivity of the vibrational bands is more pronounced in the solid state. Line width effects, peak splitting, and frequency shifts are all observed in the solid. DFT calculations have been used to help interpret the distribution of *n*-heptane conformers and its effect on the IR spectra. The energetic ordering agrees with the trend previously inferred on the basis of molecular mechanics estimates.[21] However, the DFT enthalpy difference between **G** and **A** is slightly greater than that usually assumed in empirical force fields, an average of 3.62 kJ mol^{-1} for chains with a single **G** and an average of $\Delta H = 3.94$ kJ mol^{-1} (± 0.01) per **G** for chains that have more than one **G**, so long as two adjacent gauche interactions do not have opposite helicity. As previously noted, when chains do have two gauche interactions of opposite helicity, one of them adopts a dihedral angle near 90°. According to the recently proposed nomenclature, such bonds are designated as ortho (**O**, as Chart 1 depicts and as used in Table 3).

The DFT results listed in Table 3 predict that 76% of the CH_2-CH_2 bonds in *n*-heptane vapor should be antiperiplanar

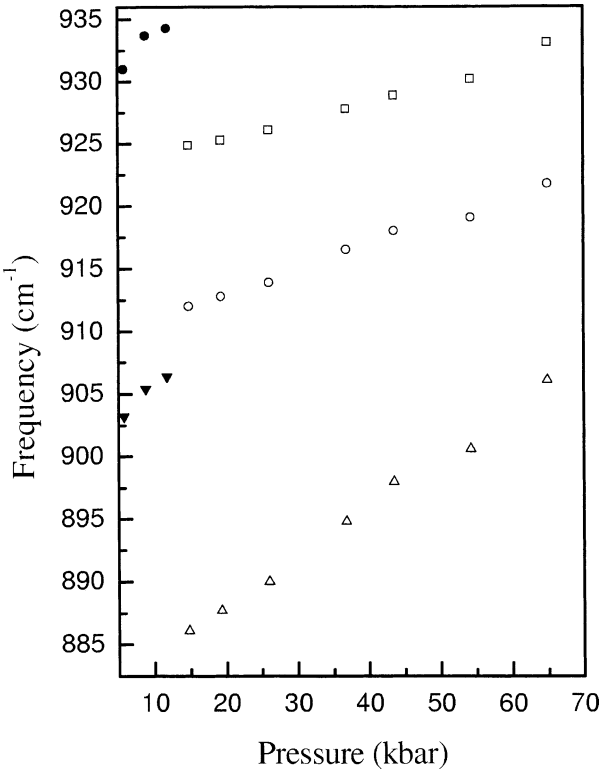

Figure 9. Infrared spectra of *n*-heptane in CH_3 rock region at various pressures.

TABLE 2: Pressure Dependence of Vibrational Frequencies in the Liquid Phase

ν_0 (cm^{-1})	$(\partial\nu/\partial P)$ (cm^{-1}/kbar)	Grüneisen param γ_i
721.3	0.35	0.00334
739.2	0.45	0.00427
773.3	0.24	0.00216
900.3	0.53	0.00411
928.2	0.55	0.00412
1467.4	0.00	0.00000

(**A**), a fraction larger than expected based on empirical force field estimates[19] and very much greater than the 45% **A** fraction determined from X-ray measurements on the liquid.[20]

We have previously noted that ab initio calculations make good predictions of low-frequency vibrations of chains and, hence, reliable estimates of 300 K vibrational entropy differences between conformers (within the limits of the harmonic approximation).[25] We turn, therefore, to the calculated enthalpy differences in order to search for the source of discrepancy between experiment and theory.

One well-precedented method of scaling from gas phase to liquid has been to suppose that the difference in ΔH between **A** and **G** becomes smaller in the liquid.[15,26,27] If we scale the calculated 0 K ΔH values between conformers by a factor of 0.6, as Table 3 lists, the ratio of antiperiplanar to gauche bonds at 300 K changes from 76:24% to 54:46%. If we suppose that an increase in hydrostatic pressure further attenuates the enthalpy differences between **A** and **G**, the relative contribution of the conformers with one **G** decreases and the proportion of the conformers with more than one **G** increases, consistent with what has been inferred from Raman measurements.

Molecular Conformation and Anharmonicity of Vibrational Modes in the Liquid Phase. The present experiments reveal IR-active modes characteristic of conformations containing gauche conformers. Figure 6 displays three CH_2/CH_3 rocking vibrations for liquid *n*-heptane (<14.9 kbar). In the fully extended conformation, only two should have the correct symmetry for electric-dipole-allowed transitions. These correspond to the broad bands seen near 725 and 775 cm^{-1} in the published gas phase and liquid IR spectra[28] (and bands reported in the Raman spectrum of the liquid[14]). A third intermediate band can be seen in the lower traces in Figure 6. This band corresponds to normal modes in the domain 749−763 cm^{-1} calculated for nearly all of the gauche-containing conformations (in a few—notably the **AG$_+$AG$_+$**, **AAG$_+$O$_-$**, and **AO-G$_+$A** conformations—the calculated IR intensity of this middle band is greater than those of the other two rocking vibrations). As Figure 7 depicts, the frequencies of all three bands increase with pressure, and the middle band disappears (along with an abrupt change in the other two band positions) when the sample crystallizes.

The effects of population changes of the different molecular conformers in the liquid are seen in the vibrational bands corresponding to C−C skeleton modes in the domain 1050−1080 cm^{-1}. The main characteristic of the pressure-induced changes in the liquid is a shift to higher frequencies, as Figure 2 summarizes. At the same time, the band near 1050 cm^{-1} becomes narrower, going from a full width at half-maximum on the order of 15 cm^{-1} at 5.8 kbar to about half that width at 11.8 kbar, as the spectra in Figure 3 depict. The intensity of this band also increases with pressure by about a factor of 1.2. The DFT calculations predict no normal mode between 1045 and 1070 cm^{-1} for the fully extended conformation (**AAAA**) nor for the one with a single 2,3-gauche bond (**GAAA**). However, two bands are predicted for this region (1053 and 1062 cm^{-1}) for the 3,4-gauche conformer (**AGAA**), and other IR-active absorptions are predicted in the region 1050−1065 for all the other conformers that have a gauche or ortho bond in that position, as listed in the last column of Table 3. A simple model can account for the increase in intensity of this band.

One plausible model for the pressure dependence of conformational equilibria is that the ΔH for **A** → **G** decreases with increasing pressure (analogous to the assumed drop in going from the vapor to the liquid phase). If the scaling factor for the DFT-calculated ΔH values is decreased from 0.6 to 0.4, the population of conformers with less than three **A**s increases by a factor of 1.31. This model for the effect of hydrostatic pressure can be compared with the estimate of Schoen et al.,[15] who examined pressure-dependent conformational changes in liquid *n*-heptane at 338 K by Raman scattering. They estimated that about 10% of the molecules are in the **AAAA** conformation at 1 atm (as compared with 11% calculated when the DFT ΔH is scaled by 0.6) and that a little less than 40% have a single **G** (as opposed to 44% calculated from DFT). If the scaling factor for the DFT-calculated ΔH values is decreased from 0.6 to 0.4, the predicted 338 K population of **AAAA** falls to 0.64 of its initial value, the population of **GAAA** plus **AGAA** drops to 0.83 of its initial value, and the population of conformers with less than three **A**s increases by a factor of 1.26. Schoen et. al. concluded that when an increase in pressure diminishes the population of **AAAA** to 0.64 of its 1 atm value, the population of **GAAA** plus **AGAA** drops to 0.75 of its 1 atm value, while the population of conformers with less than three **A**s increases by a factor of 1.22.

The DFT calculations of IR absorption intensity (weighted by 300 K conformer populations) predict that the oscillator strength of absorptions in the 1050−1065 cm^{-1} region should rise by a factor of 1.13, the net result of an increase in the fraction of conformers with less than three **A**s at the same time as the **AGAA** population diminishes. Thus, a model that

TABLE 3: DFT Results for *n*-Heptane Conformers (B3LYP/6-31G*), Summarizing Relative Electronic and Zero Point Energies (kJ mol^{-1}); Relative Vibrational Entropies (J mol^{-1} K^{-1}), Symmetry Corrections to the Entropy (assuming equal mixtures of nonsuperimposable mirror images); 300 K Boltzmann Weights for Different Scalings of Calculated Zero K Enthalpies Relative to the Fully Extended (AAAA) Chain; and the DFT Calculated Frequencies (cm^{-1}) in the 1050−1065 cm^{-1} Domain for Conformers with at Least One Gauche or Ortho C_3-C_4 Bond.

conformation	ΔE^{el}	ΔZPE	ΔS_{vib}	symmetry correction	Boltzmann weight ΔH	Boltzmann weight $0.6\Delta H$	Boltzmann weight $0.4\Delta H$	DFT freqs
AAAA	0	0	0	$-R$ ln 2	0.267	0.129	0.080	
GAAA	3.57	0.08	0.21	$+R$ ln 2	0.252	0.218	0.182	
AGAA	3.74	−0.15	0.89	$+R$ ln 2	0.281	0.242	0.200	1053, 1062
AG_+AG_-	7.57	0.43	1.83	$+R$ ln 2	0.053	0.092	0.109	1050
AG_+AG_+	7.23	0.62	−0.71	$+R$ ln 2	0.042	0.071	0.083	1056
AAG_+G_+	6.90	0.96	−3.32	$+R$ ln 2	0.031	0.052	0.060	1064
G_+AAG_-	7.20	0.49	0.32	0	0.025	0.042	0.048	
AG_+G_+A	7.15	0.71	−0.94	0	0.020	0.035	0.041	1055
G_+AAG_+	7.13	1.07	−3.95	0	0.012	0.023	0.029	
AO_-G_+A	13.86	0.36	−1.39	$+R$ ln 2	0.002	0.015	0.027	1060, 1063
AAG_+O_-	14.02	0.35	1.30	$+R$ ln 2	0.004	0.019	0.037	1051, 1065
AAO_+G_-	14.11	0.13	1.35	$+R$ ln 2	0.004	0.020	0.038	1061, 1065
$AG_+G_+G_+$	10.46	1.22	−3.45	$+R$ ln 2	0.006	0.021	0.032	1057, 1061
$G_+AG_+G_+$	10.49	1.34	−3.94	$+R$ ln 2	0.006	0.021	0.032	1053

[a] For explanation of abbreviations, see Chart 1 and the text.

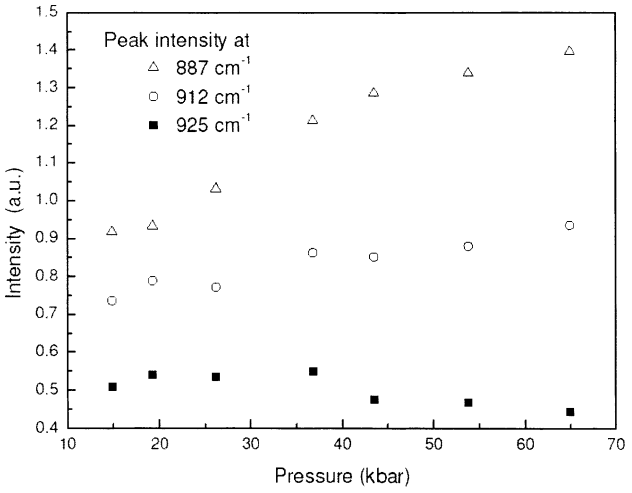

Figure 10. Pressure dependence of the peak intensity in CH_2 rock and twist region.

interprets the effect of increasing pressure simply in terms of a reduction in the conformational enthalpy difference agrees reasonably well with experimental measurements.

The pressure dependence of the conformer population in *n*-alkane molecules has been studied by several authors.[3,12,15] They have concluded that globular conformations with some gauche bonds become preferable at high pressures in the liquid, rather than the more extended structures that represent the lowest energy conformations for isolated molecules. A qualitative explanation can be presented as follows. Increasing the number of gauche bonds gives the molecule a more globular shape. The excluded volumes for the globular conformations of alkyl molecules are smaller than those of the more rodlike, extended conformations.[15] If, under high pressure, the decrease of the conformational energy by hydrostatic compression outweighs the cost of forming additional gauche bonds, an increased fraction of molecules will adopt conformations with increased numbers of gauche (or ortho) bonds. Some normal modes (such as the band near 1055 cm^{-1}) are characteristic of more globular conformations. Other internal degrees of freedom (such as the localized methyl rocking modes) are less sensitive to changes of molecular conformation, and the pressure dependence of those modes reflects the anharmonicity of the vibrations rather than conformational change. The pressure dependences of the vibrational mode frequencies in the solid phase are fit to eq 1

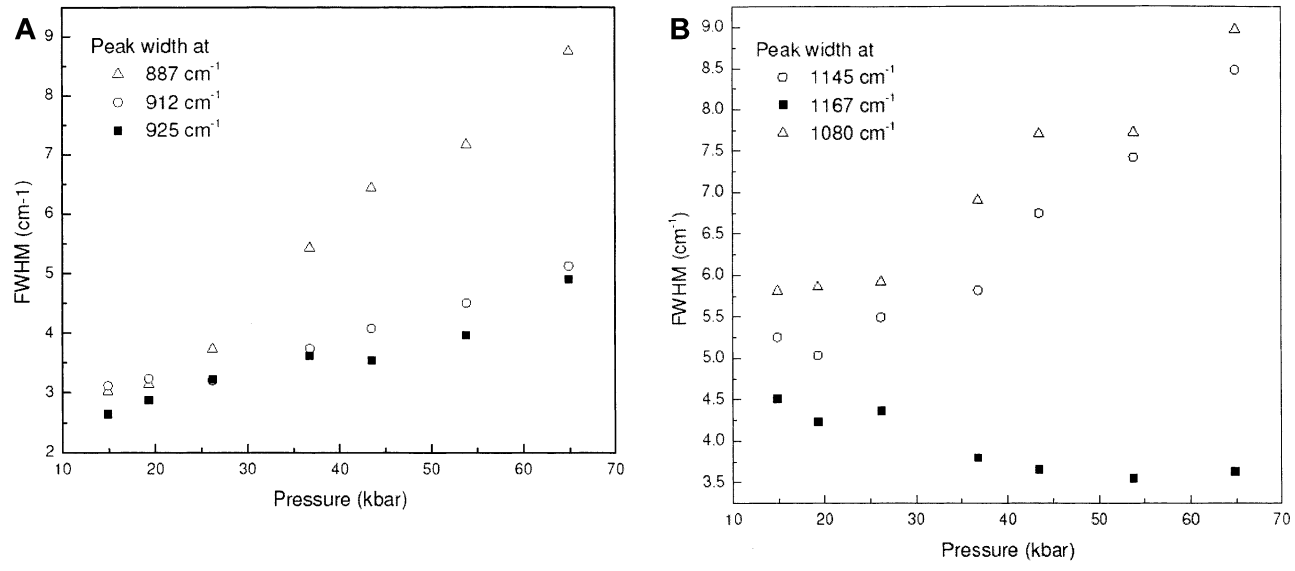

Figure 11. Pressure dependence of the full width at half-maximum (fwhm) in (a) CH_2 rock and twist region and (b) C−C stretching region.

$$\nu(P) = \nu_0 + \left(\frac{\partial \nu}{\partial P}\right)_P = 0P \quad (1)$$

where $\nu(P)$ and ν_0 are the frequency of the vibrational mode at pressure, P, and the frequency of the vibrational mode at zero pressure, respectively. The pressure derivatives are in the range of 0−0.6 cm^{-1} $kbar^{-1}$, as listed in Table 2. Alternatively, a Grüneisen parameter, γ, is often used to evaluate the anharmonicity of vibrational modes in the solid phase, based on the lattice dynamics, whereas the pressure-induced frequency change (ν_p/ν_0) is related to the corresponding bulk volume change (V_p/V_0) as $(\nu_p/\nu_0) = (V_p/V_0)^{-\gamma}$. For molecular liquids, a pseudo-Grüneisen parameter has been used to explore the relationship between the thermodynamic properties, a parameter that can be derived based on the clustering of liquid molecules.[29−31] The relatively small pressure dependences of the peak frequencies in liquid *n*-heptane merely imply that the localized molecular vibrations investigated in this study have small anharmonicities with respect to compression of intermolecular coordinates.

Phase Transitions. *(i) Liquid−Solid Phase Transition.* As Figures 1, 4, 6, and 8 show, the infrared spectrum of *n*-heptane undergoes characteristic changes associated with a liquid−solid phase change between 11.8 and 14.9 kbar. The spectra in the liquid phase show broad bands consisting of the superposition of the several vibrational modes. *n*-Heptane can adopt 13 different molecular conformations (of which we have performed DFT calculations on the 11 lowest lying) if we neglect conformations with sequences of gauche−ortho bonds.[27] All these conformers are thermally populated, and each of the conformers with different vibrational modes contributes to the infrared spectrum in the liquid to give inhomogeneously broadened peak profiles. In contrast, the spectra above 14.9 kbar have relatively sharp bands with single peak features.

n-Alkane chains in the crystal are known to have fully extended (all **A**) conformations; hence, the spectra of the solid at high pressure is attributed to vibrations of the **AAAA** conformer.[24] The discontinuities of the spectral features between liquid and solid are also seen from the pressure-dependent vibrational frequencies shown in Figures 2, 5, 7, and 9. Due to changes in the populations of the conformer states at the phase transition, the vibrational bands for the liquid and solid do not necessarily correspond to the same vibrational mode for the same conformer. In the solid phase, the IR bands correlated with a bending−twisting mode (1400−1550 cm^{-1}) show a single peak feature, for which splitting was not observed over the pressure range of this study.

(ii) Solid−Solid Phase Transition. Two peaks in the 1400−1550 cm^{-1} region are assigned to mixed asymmetric CH_3 and CH_2 bending modes, which, in turn, each split into two additional peaks between 26 and 36 kbar, as shown in Figure 4. No other bands show a similar splitting in this same pressure range. However, the line width and the intensity of some peaks show changes in the slope and/or discontinuity of the pressure dependence in the same pressure range where the peaks near 1450 and 1463 cm^{-1} were observed to begin splitting, as illustrated in Figures 10 and 11. These changes suggest the existence of a solid−solid phase transition in this pressure range. The line width of the antisymmetric CH_3 rocking mode around 886 cm^{-1} increases rapidly above 36 kbar, while the line width of the symmetric CH_3 rocking mode near 912 cm^{-1} shows less evident changes in this pressure range. In addition, the intensity of the symmetric CH_3 rocking mode has a relatively large increase near 30 kbar, yet there is little change in the intensity of the corresponding antisymmetric CH_3 rocking mode. The nature of the solid−solid phase transition is not yet clear, including questions regarding the order of the transition, whether there are soft modes, and, if so, where in the Brillouin zone they may be found. Intermolecular phonon modes can be much more sensitive to structural changes of the host matrix, and pressure-dependent far-IR experiments will help to confirm the proposed polymorphic phase change.

Acknowledgment. E.L.C. acknowledges financial support of this research under National Science Foundation Grant CHE-9714886. T.H.M. acknowledges financial support of this research under NSF Grant CHE-9983610. E.L.C. also acknowledges an Air Force Office of Scientific Research Grant F49620-98-1-0475 used to purchase the FTIR.

References and Notes

(1) Neumann, M. A.; Johnson, M. R.; Radaelli, P. G. *Chem. Phys.* **2001**, *266*, 53.

(2) Dirand, M.; Bouroukba, M.; Chevallier, V.; Petitjean, D. *J. Chem. Eng. Data* **2002**, *47* 115−143. Chevallier, V.; Petitjean, D.; Ruffer-Meray, V.; Dirand, M. *Polymer* **1999**, *40*, 5953.

(3) Wong, P. T. T.; Chagwedera, T. E.; Mantsch, H. H. *J. Chem. Phys.* **1987**, *87*, 4487.

(4) Pratt, L. R.; Hsu, C. S.; Chandler, D. *J. Chem. Phys.* **1977**, *68*, 4202. Montgomery, J. A., Jr.; Holmgren, S. L.; Chandler, D. *J. Chem. Phys.* **1980**, *73*, 3688.

(5) McGann, M. R.; Lacks, D. J. *J. Phys. Chem. B* **1999**, *103*, 2796.

(6) Aljibury, A. L.; Snyder, R. G.; Strauss, H. L.; Raghavachari, K. *J. Chem. Phys.* **1986**, *84*, 6872.

(7) Streitwieser, A. G., Jr.; Heathcock, C. H. In *An Introduction to Organic Chemistry*; Macmillan Publishers: New York, 1976; p 56.

(8) Trudell, J. R.; Hubbell, W. L.; Cohen, E. N. *Biochim. Biophys. Acta* **1973**, *291*, 328.

(9) Wong, T. T. *Annu. Rev. Biophys. Bioeng*. **1984**, *13*, 1.

(10) Bassett, D. C. In *Principles of Polymer Morphology*; Cambridge University: New York, 1981.

(11) Snyder, R. G.; Strauss, H. L.; Alamo, R.; Mandekern, L. J. *J. Chem. Phys.* **1993**, *100*, 5422.

(12) Kato, M.; Taniguchi, Y. *J. Chem. Phys.* **1991**, *94*, 4440.

(13) Snyder, R. G. *J. Chem. Phys.* **1982**, *76*, 3342. Kent, S.; Scherer, J. R.; Snyder, R. G. *J. Chem. Phys.* **1980**, *73*, 2599.

(14) Cho, Y.; Kobayashi, M.; Tadokoro, H. *J. Chem. Phys.* **1986**, *84*, 4636.

(15) Schoen, P. E.; Priest, R. G.; Sheridan J. P.; Schnur, J. M. *J. Chem. Phys.* **1979**, *71*, 317.

(16) Wong, P. T. T.; Mantsch, H.; Snyder, R. G. *J. Chem. Phys.* **1983**, *79*, 2369.

(17) Grall, G.; Feis, A.; Friedrich, J. *J. Chem. Phys.* **1992**, *97*, 5403. Friebel, J.; Friedrich, J.; Suisalu, A.; Kikas, J.; Kuznetsov, An.; Laisaar, A.; Leiger, K. *J. Chem. Phys.* **1988**, *108*, 1830.

(18) Michl, J. *Acc. Chem. Res.* **2000**, *33*, 821.

(19) Bonham, R. A.; Bartell, L. S.; Kohl, D. A. *J. Am. Chem. Soc.* **1959**, *81*, 4765.

(20) Habenschuss, A.; Narten, A. H. *J. Chem. Phys.* **1990**, *92*, 5692.

(21) Tsuzuki S.; Schafer L.; Goto H.; Jemmis E. D.; Hosoya, H.; Siam, K.; Tanabe, K.; Osawa, E. *J. Am. Chem. Soc.* **1991**, *113*, 4665.

(22) Merrill, L.; Bassett, W. A. *Rev. Sci. Instrum*. **1974**, *45*, 290.

(23) Snyder, R. G.; Schachtschneider, J. H. *Spectrochim. Acta* **1963**, *19*, 85.

(24) Schachtschneider, J. H.; Snyder, R. G. *Spectrochim. Acta* **1963**, *19*, 117.

(25) Kohler, B. E.; Morton, T. H.; Nguyen, V.; Shaler, T. A. *J. Phys. Chem. A* **1999**, *103*, 2302.

(26) Snyder, R. G.; Kim, Y. *J. Phys. Chem.* **1991**, *95*, 602.

(27) Flory, P. J. In *Statistical Mechanics of Chain Molecules*; John Wiley & Sons: New York, 1969.

(28) Pouchert, C. J. In *Aldrich Library of Infrared Spectra*, 3rd ed.; Aldrich Chemical Co.: Milwaukee, WI, 1981.

(29) Knopoff, L.; Shapiro, J. N. *Phys. Rev. B*: *Condens. Matter Mater. Phys.* **1970**, *10*, 3893.

(30) Tandon, U. S.; Pandey, S. K. *Phys. Lett.* **1972**, *41A*, 161.

(31) Lopes, J. N. C.; Rebelo, R. P. N.; Jancso, G. *J. Mol. Liq*. **1992**, *54*, 115.